ROBUST CONTROL OF MULTI-AXIS SHAKING SYSTEM USING μ-SYNTHESIS

Y. Uchiyama [*], **M. Mukai** [**], **M. Fujita** [**]

[*] *IMV CORPORATION, Itami 664-0847, Japan*
[**] *Department of Electrical and Electronic Engineering, Kanazawa University, Kanazawa 920-8667, Japan*

Abstract: The application of the two-degree-of-freedom (2DOF) control to the electrodynamic multi-axis shaking system that is not permitted to employ the iteration control method is presented. A transformation matrix is used to remove a redundancy. The redundancy arises from the fact that the 6DOF shaking table is composed of 8-shakers. Furthermore, the influences of the specimen and the cross-coupling term is considered, and a robust controller is designed using μ-synthesis. Lastly, the good performance of the controller by experiment using an actual equipment with the resonant specimen is confirmed.

Keywords: Robust control, Control applications, Vibration control, μ-Synthesis, Two-degree-of-freedom control, Multivariable feedback control, Actuators

1. INTRODUCTION

The multi-axis shaking tables which can replicate an actual situation have come into wide use recently. An electro-hydraulic shaker generally was used for a large-scale multi-axis shaking table. On the other hand, it has been known that an electrodynamic shaker has the some good features. Thus, when the multi-axis shaking table is consisted of electrodynamic shakers, a more accurate vibration test can be realized.

The controller of the multi-axis shaking system is required to provide not only stable control, but also good replication of the reference waveform. However, when the mass of a specimen cannot be ignored in comparison with that of the shaking table, the interaction between the table and the specimen becomes significant. As a result of this interaction, the transfer function of the shaking system takes on an antiresonant characteristic at the resonant frequency of the specimen and control becomes more difficult. To avoid this difficulty, existing controllers usually employ an open-loop method using iterative compensation by repeating excitations. However, the need for a new method in which iteration control is unnecessary is increasing in several cases.

Also, like the simulation of soil-structure interaction effects (Konagai and Ahsan, 2002), an experimental method, in which a vibration test and a computer simulation are combined, tends to increase. It is necessary to control a shaker in real time without being late for the computer simulation. However, the conventional controller is based on feedforward control using FFT and can update the drive signal only per the frame time of FFT. Therefore, it is not easy to employ the conventional controller in this method.

In regard to the realization of above mentions, for example, MCS (Minimal Control Synthesis) algorithm, one of the model reference adaptive control, has been successfully applied (Stoten and Gomez, 1998), and so on. On the other hand, like the instance of Lundström *et al.* (1999), a 2DOF controller is often used for its advantage of

convenience in that the design of system stability and the control performance can be treated independently. In our previous study (Uchiyama and Fujita, 2002), a 2DOF controller using μ-synthesis is applied to the multi-axis electrodynamic shaking system. Incidentally, because of ignoring the cross-coupling problem among every shaker, influences of the cross-coupling term appear in response signals. For convenience, an adaptive filter is introduced to attenuate the influences. However, the influences are inevitably increased by the specimen which is put on the table, and it indicates that the control of the cross-coupling term is explicitly needed.

In this paper, a multi-axis controller applied to the cross-coupling control is used. In relation to a rate force and a table size, it is often the case that the system is composed of multiple shakers over the degree of freedom of the table motion. In this case, a redundancy exists, and so the gain of the controller which is designed in this system is often enlarged. Then to remove the redundancy, a transformation matrix (Maekawa *et al.*, 1993) is introduced. Additionally, a controller is designed to maintain robust stability and performance against the influences of the specimen and the cross-coupling term.

The rest of the paper is organized as follows. In section 2 a mathematical model and uncertainty weighting function for the system are introduced. A feedback controller is designed using μ-synthesis and a 2DOF controller is constituted in section 3. Section 4 provides some experimental results. Finally, in section 5, the paper is summarized.

2. MULTI-AXIS SHAKING SYSTEM MODEL

In this section, the outline of the multi-axis shaking system is explained, and a nominal model and an uncertainty weighting function are introduced.

2.1 Outline of multi-axis shaking system

The multi-axis shaking system shown in Fig. 1 is considered. This shaking system is composed of two shakers along the X,Y-axes and four shakers along the Z-axis, so it is composed of eight shakers in total. The electrodynamic shaker is based on the principle that an electrodynamic force is generated in proportion to an electric current applied to a coil which exists in a magnetic field. A table is connected to shakers by spherical bearings, and the shaking table can move smoothly with 6 degrees of freedom, that is, 3 degrees of freedom of translational motion and 3 degrees of freedom of rotational motion. Because of the difficulty of measuring the table displacement during excitation, the armature displacement of a shaker is measured using a laser displacement sensor. This system has 8-inputs to the amplifiers of shakers and 8-outputs from the displacement sensors.

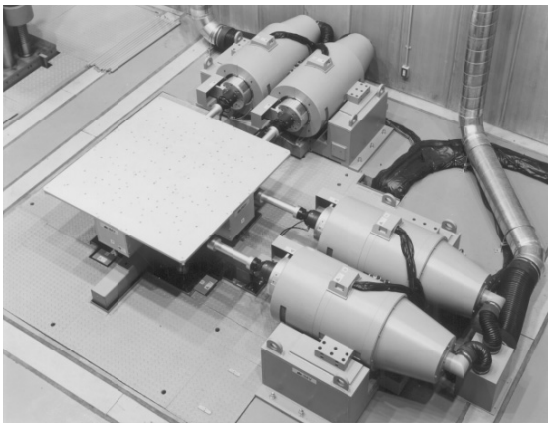

Fig. 1. Overview of multi-axis shaking system.

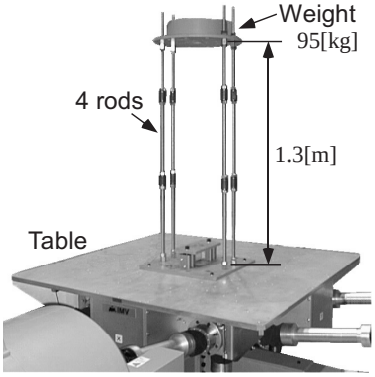

Fig. 2. Overview of the specimen.

A 95kg specimen is supported by 4 rods of 1.3m length, as shown in Fig. 2, and is put on the table. The first-order resonant frequency of the specimen is approximately 2.0Hz. However, as an accurate value of the resonance characteristic is unknown, it is assumed that the resonant frequency exists in the 1.76∼2.24Hz frequency band.

2.2 Nominal model

It is assumed that the coupling systems are shown as vibration system of single degree of freedom and the influence of the test piece mainly occur the rotary motion around X,Y-axes of the shaking table. The mathematical model of the multi-axis shaking system with the test piece is expressed as

$$\dot{x}_{wl} = A_s x_{wl} + B_s u_s \tag{1}$$

$$y_s = C_s x_{wl} \tag{2}$$

$$\begin{aligned} x_{wl} = [&x_{s1}, \ldots, x_{s8}, X_T, Y_T, Z_T, \theta_{XT}, \theta_{YT}, \theta_{ZT}, \\ &\theta_{XL}, \theta_{YL}, I_{11}, \ldots, I_{18}, \dot{x}_{s1}, \ldots, \dot{x}_{s8}, \\ &\dot{X}_T, \dot{Y}_T, \dot{Z}_T, \dot{\theta}_{XT}, \dot{\theta}_{YT}, \dot{\theta}_{ZT}, \dot{\theta}_{XL}, \dot{\theta}_{YL}\Big]^T \end{aligned}$$

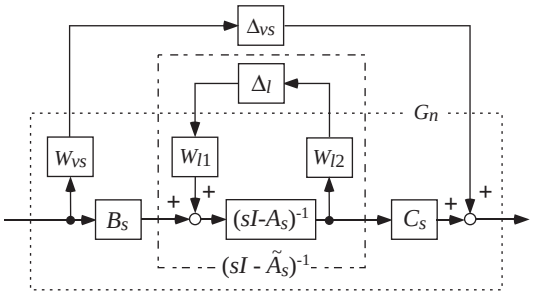

Fig. 3. Perturbation structure.

$$u_s = [u_{s1}, u_{s2}, \ldots, u_{s8}]^T$$
$$y_s = [x_{s1}, x_{s2}, \ldots, x_{s8}]^T,$$

where x_{si} are armature displacement, X_T, Y_T, Z_T, $\theta_{XT}, \theta_{YT}, \theta_{ZT}$ are position and attitude of the table gravity, θ_{XL}, θ_{YL} are specimen attitude, I_{1i} are current of the drive coil. By comparing the measured value with the simulated value, the nominal values are determined. Also, the characteristic of antialiasing filter is added to (1), (2), and that model is defined as the nominal model, which has 56 states.

2.3 Modeling uncertainty

In this study, parametric state-apace uncertainty (Skogestad and Postlethwaite, 1996), Δ_l, is employed to represent the influence of the specimen, and an unstructured additive perturbation, Δ_{vs}, is used for the uncertainties of each shaker, as shown in Fig. 3. The model enclosed within the dotted line is G_n. First, the perturbation of the test piece is considered. Because of the perturbation range of resonant frequency, the stiffness coefficient, $\tilde{K}_l$, is shown as

$$\tilde{K}_l = K_l + \delta_l w_l, \ |\delta_l| \leq 1. \tag{3}$$

An uncertain state-space parameter, $\tilde{A}_s$, may be written as

$$\tilde{A}_s = A_s + \delta_l A_{wl}, \tag{4}$$

where A_{wl} is composed by w_l, which may enter into the matrix in several places. And then δ_l is collected in a diagonal matrix, Δ_l, Eq. (4) is rearranged as

$$\tilde{A}_s = A_s + W_{l2}\Delta_l W_{l1}, \tag{5}$$

where

$$\Delta_l = \begin{bmatrix} \delta_l & 0 \\ 0 & \delta_l \end{bmatrix}$$
$$W_{l2} = [A_{wl}(k,12) \ \ A_{wl}(k,13)], \ k = 1, \ldots, 56$$
$$W_{l1} = \begin{bmatrix} \mathbf{0}_{1\times11} & 1 & 0 & 0 & -1 & 0 & \mathbf{0}_{1\times19} & w_{rat} & 0 \\ \mathbf{0}_{1\times11} & 0 & 1 & 0 & 0 & -1 & \mathbf{0}_{1\times19} & 0 & w_{rat} \end{bmatrix}$$

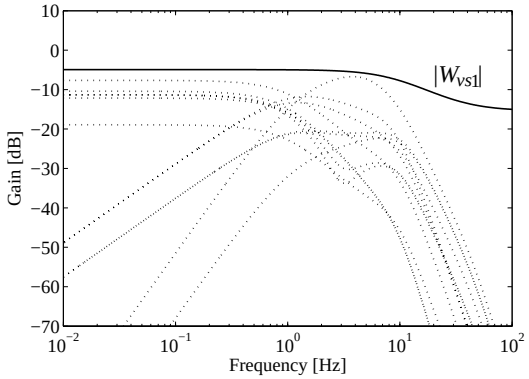

Fig. 4. Uncertainties (dotted) and weighting function W_{vs1} (solid).

$$\begin{bmatrix} 0 & -w_{rat} & 0 & \mathbf{0}_{1\times16} \\ 0 & 0 & -w_{rat} & \mathbf{0}_{1\times16} \end{bmatrix},$$

and w_{rat} is the ratio of dividing a perturbation range of the damping factor by w_l.

Next, additional uncertainty in the parameter perturbations of each shaker is considered. For example, the additional uncertainties of X1 shaker are shown by dotted lines in Fig. 4. Here, the magnitude of the weighting function, W_{vs1}, is chosen to cover all the perturbations as follows:

$$W_{vs1} = \frac{0.17(s+200)}{s+60}. \tag{6}$$

The weighting function, $W_{vs2\sim8}$, of X2∼Z4 shaker is obtained by the same idea, and W_{vs} is given by

$$W_{vs} = \mathrm{diag}\,(W_{vs1}, W_{vs2}, \ldots, W_{vs8}). \tag{7}$$

Also, additional perturbations is considered for each shaker, and Δ_{vs} is shown as follow:

$$\Delta_{vs} = \mathrm{diag}\,(\Delta_{vs1}, \Delta_{vs2}, \ldots, \Delta_{vs8}). \tag{8}$$

3. CONTROLLER DESIGN

The design of the controller of an electrodynamic shaker is carried out using MATLAB.

3.1 Control objectives

The following items is set to the control objectives for the multi-axis shaking system.

- Stabilize the system even when an uncertainty exists.
- Maintain the performance wherein a disturbance is damped and the seismic wave is replicated well.

The transformation matrix is introduced in order to remove the redundancy of the system. A controller is designed to maintain robust stability

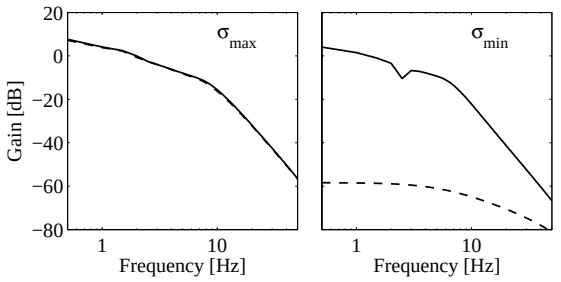

Fig. 5. $\sigma_{\max}$ and $\sigma_{\min}$ of each plant models.

against the uncertainty model. Moreover, it is desired that a controller maintains a good performance against this uncertainty. Thus, the controller for this system is designed by μ-synthesis (Fujita *et al.*, 1995). A 2DOF controller is fabricated to improve the transient response.

3.2 Transformation matrix

The matrix, T_{ts}, for transforming the 6DOF signals to the input signals of the shakers is obtained by the geometrical relation of the conjunction points between the shakers and the shaking table. T_{ts} is defined as follow

$$T_{ts} = \begin{bmatrix} 1 & 0 & 0 & 0 & -h_{z1} & -h_{y1} \\ 1 & 0 & 0 & 0 & -h_{z2} & h_{y2} \\ 0 & 1 & 0 & h_{z3} & 0 & -h_{x3} \\ 0 & 1 & 0 & h_{z4} & 0 & h_{x4} \\ 0 & 0 & 1 & h_{y5} & h_{x5} & 0 \\ 0 & 0 & 1 & -h_{y6} & h_{x6} & 0 \\ 0 & 0 & 1 & -h_{y7} & -h_{x7} & 0 \\ 0 & 0 & 1 & h_{y8} & -h_{x8} & 0 \end{bmatrix}, \tag{9}$$

where h_{xi},h_{yi},h_{zi} are the length from each conjunction points to X,Y,Z-axes. The inverse transformation of T_{ts} employs a pseudoinverse matrix, T_{ts}^{+}. This matrix is added to (1), (2), and the plant model can be shown as

$$\dot{x}_{wl} = A_s x_{wl} + B_s T_{ts} u_{6dof} \tag{10}$$

$$y_{6dof} = T_{ts}^{+} C_s x_{wl}, \tag{11}$$

$$u_{6dof} = [u_X, u_Y, u_Z, u_{\theta_{XT}}, u_{\theta_{YT}}, u_{\theta_{ZT}}]^T$$

$$y_{6dof} = [X'_T, Y'_T, Z'_T, \theta'_{XT}, \theta'_{YT}, \theta'_{ZT}]^T,$$

where u_{6dof} is the input voltage to the amplifier, y_{6dof} is the estimated value of the table position and attitude. The maximum singular values, $\sigma_{\max}$, and the minimum singular values, $\sigma_{\min}$, of the transfer function are shown in Fig. 5, where the solid lines show the characteristic of the plant model of (10), (11), the dashed lines show the original plant model of (1), (2). Comparing the both characteristic of the plant model, the difference of $\sigma_{\max}$ and $\sigma_{\max}$ is small in the case of using the transformation matrix. Then, it appears that the redundancy of the system can be removed by using the transformation matrix.

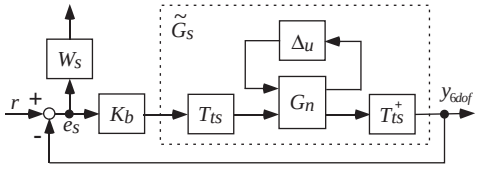

Fig. 6. Feedback structure.

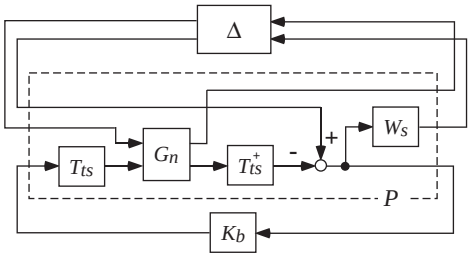

Fig. 7. Generalized plant.

3.3 μ-synthesis

Let us consider the feedback structure shown in Fig. 6, where r is a control reference, e_s is a control error, K_b is the feedback controller, $\Delta_u = \mathrm{diag}(\Delta_{vs}, \Delta_l)$. A weighting function, W_s, for the replication performance of the reference signal is considered. For a precise replication of a seismic wave, it is needed that the gain of the low-frequency band is enlarged, because the main frequency components of a seismic wave exists in the low-frequency band. Then, W_s is chosen

$$W_s = \mathrm{diag}(W_{ss}, W_{ss}, W_{ss}, W_{ss}, W_{ss}, W_{ss}) \tag{12}$$

$$W_{ss} = \frac{10 \cdot \alpha \cdot 0.175 \cdot 2\pi}{s + 0.175 \cdot 2\pi} \cdot \frac{0.35 \cdot 2\pi}{s + 0.35 \cdot 2\pi} \cdot \left(\frac{1.75 \cdot 2\pi}{s + 1.75 \cdot 2\pi} \right)^2,$$

where, α is the adjustment parameter. α can be enlarged as long as the uncertainty is satisfied. Here, the adjustment parameter α is set 1.5.

As stated above, the design objective for stability and control performance is formalized as the requirements for a closed-loop transfer function with weighting functions. Therefore, the generalized plant, P, which is shown in Fig. 7, is constructed to make the control objectives fit the μ-synthesis framework. Here, the block structure, Δ, of the uncertainty is defined as

$$\begin{aligned} \Delta := \{ & \mathrm{diag}\left(\Delta_{vs1}, ..., \Delta_{vs8}, \delta_l, \delta_l, \Delta_{perf}\right), \\ & \Delta_{vs1}, ..., \Delta_{vs8} \in \mathcal{C}^{1\times 1}, \delta_l \in \mathcal{C}^{1\times 1}, \\ & \Delta_{perf} \in \mathcal{C}^{6\times 6} \}, \end{aligned} \tag{13}$$

where $|\Delta_{vsi}| \leq 1$, $\|\Delta_{perf}\|_\infty \leq 1$, and Δ_{perf} is a fictitious uncertainty block for considering robust performance. Next, consider this generalized plant, P, partitioned as

$$P = \begin{bmatrix} P_{11} & P_{12} \\ P_{21} & P_{22} \end{bmatrix}. \tag{14}$$

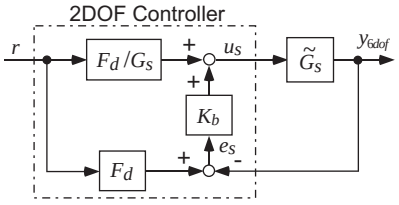

Fig. 8. Block diagram of 2DOF control.

LFT on P by K_b is defined as follows:

$$F_l(P, K_b) := P_{11} + P_{12}K_b(I - P_{22}K_b)^{-1}P_{21}. \quad (15)$$

The robust performance condition is equivalent to the following structured singular value μ.

$$\sup_{\omega \in \mathcal{R}} \mu_\Delta \left(F_l(P, K_b)(j\omega)\right) < 1 \quad (16)$$

Since the controller satisfies this condition, D-K iteration procedure is employed. The controller which satisfies Eq. (16) is obtained after 4 iterations, and the degree of this controller has been reduced from 168 states to 31 states.

3.4 Construction of 2DOF controller

Due to improvement of the transient response, the 2DOF controller is constructed as shown in Fig. 8, where F_d is reference model. An H_2 optimal controller (Sugie and Tanai, 1994) is employed as the feedforward controller. The cost function is considered as follow

$$J_{FF} = \left\| \begin{array}{c} \dfrac{1}{s}\left(1 - G_{yr}\right) \\ \rho G_{ur} \end{array} \right\|_2 . \quad (17)$$

where G_{yr} is the transfer characteristic from r to y_s, G_{ur} is the transfer characteristic from r to u_s. In this reference, the instability eigenvalue by the integration weight is neglected, and the solution is obtained explicitly. The first term of (17) shows the quantity of the tracking error to a step input and good tracking performance is obtained by decreasing the quantity. The second term shows the energy of the control input to a impulse input and the control input is saved by decreasing the energy. ρ is the weighting parameter for having the trade-off between the first term and the second term. In this case, since the bandwidth of F_d, is set at about 10Hz, ρ has been chosen $\rho = 0.001$. The degree of this controller has been reduced from 62 states to 28 states.

4. EXCITATION EXPERIMENT

The performance of the designed controller is confirmed by experiments using the resonant specimen shown in Fig. 2. The controller is discretized via the Tustin transform at the sampling frequency of 1KHz.

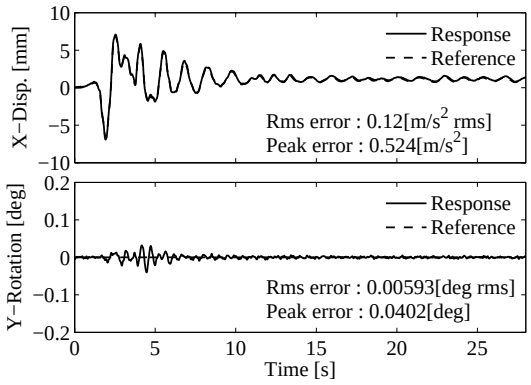

Fig. 9. Results of uncross-coupled control: 0.75Hz.

4.1 Setting of experiment

In this experiment, an excitation whereby a reference signal of the measurement wave is input in only the X-axis direction is executed. However, even if an excitation is executed in the X-axis direction, a rotary motion around the Y-axis occurs due to the influence of interference by the specimen. It is required that the controller suppresses this rotary motion. The control performance is evaluated by the result of the transient response at that excitation. The influence of the specimen is adjusted by changing the dominant frequency component of the reference waveform.

For evaluating an effect of multi-axis control, the previous controller which ignores the cross-coupling term is used. In this case, SISO controllers are designed for each shaker.

4.2 Control results

First, the control performance is confirmed when the influence of the specimen is small. Since the influence of the specimen is reduced, the main frequency components of a reference waveform differ from the resonant frequency which had been set at 0.75Hz. The results of SISO controls are shown in Fig. 9, and the results of the proposal method are shown in Fig. 10. In the rotary motion around the Y-axis which is main evaluation item of this experiment, both results are successfully controlled. The waveform replication of X-axis shown in Fig. 10 does not yield a good performance compared to Fig. 9. The reason for this difference is that the bandwidth of F_d and the adjustment parameter of W_s are not same. Then, it appears that the performance is improved by the proper choice of the parameters.

Next, in an experiment using a waveform which has its main frequency components in the neighborhood of resonant frequency, a rotary motion occurs due to the influence of the specimen. The SISO controllers cannot suppress the undesired

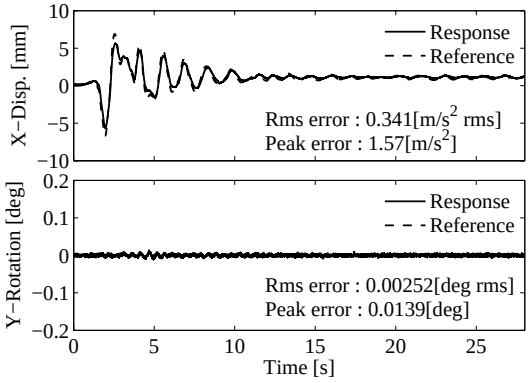

Fig. 10. Results of the proposal control: 0.75Hz.

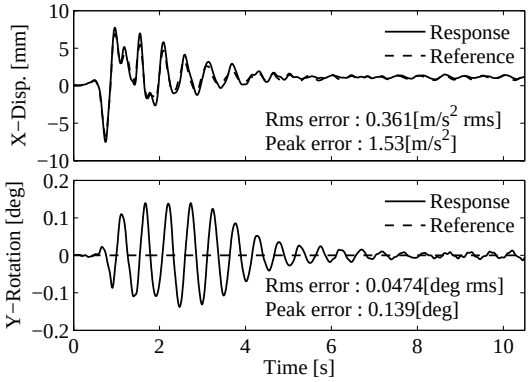

Fig. 11. Results of uncross-coupled control: 2Hz.

motion, as shown in Fig. 11. The results of the proposal controller is shown in Fig. 12. Comparing the results of Fig. 12 with Fig. 11, it is confirmed that the rotary motion can be effectively suppressed by the proposal method. It appears that the effect is obtained because of the control of the cross-coupling term. In X-axis, the response signal in Fig. 11 overshoots the reference, whereas the proposal method yields similar performance with the result of Fig. 10.

Also, the rms error, which is rms value of the error waveform, and the peak error are written in the control results respectively. It is found that both errors of the rotary motion are especially decreased to about one-third because of using the proposal controller. These results support the conclusion that this method is useful.

5. CONCLUSION

In this study, It has been assumed that a conventional open-loop method using iterative compensation by repeating excitations can not be employed for the electrodynamic multi-axis shaking system, and the controller has been constructed for such a situation. The proposal method has been considered that the cross-coupling term is controlled and the redundancy of the system is removed. Comparing the proposal method with

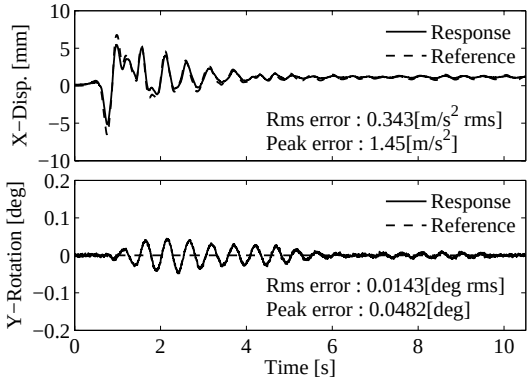

Fig. 12. Results of the proposal control: 2Hz.

the uncross-coupled controller, it has been shown that the good performance of this controller is ascertained by the experiment. Although applying to other specimens should be needed, it would be considered that the application of this method to multi-axis shaking systems is useful.

REFERENCES

Fujita, M., T. Namerikawa, F. Matsumura and K. Uchida (1995). μ-synthesis of an electromagnetic suspension system. *IEEE Transactions on Automatic Control* **40**, 530–536.

Konagai, K. and R. Ahsan (2002). Simulation of nonlinear soil-structure interaction on a shaking table. *Journal of Earthquake Engineering* **6**, 31–51.

Lundström, P., S. Skogestad and J. C. Doyle (1999). Two-degree-of-freedom controller design for ill-conditioned distillation process using μ-synthesis. *IEEE Transactions on Control Systems Technology* **7**, 12–21.

Maekawa, A., C. Yasuda and T. Yamashita (1993). Application of h_∞ control to a 3-d shaking table (in japanese). *Transactions of the SICE of Japan* **29**, 1094–1103.

Skogestad, S. and I. Postlethwaite (1996). *Multivariable Feedback Control: Analysis and Design*. John Wiley & Sons.

Stoten, D. P. and E. Gomez (1998). Recent application results of adaptive control on multi-axis shaking tables. *Proceedings of the 6th SECED International Conference, Seismic Design Practice into the Next Century* pp. 381–387.

Sugie, T. and Y. Tanai (1994). h_2/h_∞ suboptimal controller design of magnetic levitation systems (in japanese). *Transactions of the SICE of Japan* **30**, 1202–1208.

Uchiyama, Y. and M. Fujita (2002). Robust control of multi-axis electro-dynamic shaking system by 2-degree-of-freedom control using μ-synthesis in feedback control (in japanese). *Transactions of the JSME* **C68**, 2680–2686.